Symmetric and asymmetric nuclear matter in the relativistic approach

H. Huber, F. Weber, and M. K. Weigel
Universität München, Am Coulombwall 1, D-85748 Garching, Germany
(Received 19 October 1994)

Symmetric and asymmetric nuclear matter is studied in the framework of the relativistic Brueckner-Hartree-Fock and in the relativistic version of the so-called Λ^{00} approximation. The equations are solved self-consistently in the full Dirac space, so avoiding the ambiguities in the choice of the effective scattering amplitude in matter. The calculations were performed for some modern meson-exchange potentials constructed by Brockmann and Machleidt. In some cases we used also the Groningen potentials. First, we examine the outcome for symmetric matter with respect to other calculations, which restrict themselves to positive-energy states only. The main part is devoted to the properties of asymmetric matter. In this case we obtain additionally to the good agreement with the parameters of symmetric matter, also a quite satisfactory agreement with the semiempirical macroscopic coefficients of asymmetric matter. Furthermore, we tested the assumption of a quadratic dependence of the asymmetry energy for a large range of asymmetries. Included is also the dependence of nucleon self-energies on density and neutron excess. For the purpose of comparison we discuss further the similarities and differences with relativistic Hartree and Hartree-Fock calculations and nonrelativistic Skyrme calculations.

PACS number(s): 21.30.+y, 21.65.+f, 24.10.Cn, 24.10.Jv

I. INTRODUCTION

The past decades have seen many successes in the application of relativistic theories to the nuclear many-body problem. Relativistic treatments have advantages in several respects, as for instance [1,2]: An extremely useful Dirac phenomenology for the description of nucleon-nucleus scattering [3], the natural incorporation of the spin-orbit force [1,2], the shift of the saturation curve from the so-called "Coester band" towards the "experimental" value [4] via a new saturation mechanism [1,2], the successful description of finite nuclei [5–8] etc. Comprehensive surveys can be found, for instance, in Refs. [1,2]. One of the primary challenges in every many-body theory is to "understand" the properties of the system in terms of the interactions between its constituents (so-called parameter-free theories). One basic attempt in this direction is the relativistic treatment in many-body approximations with dynamical two-body correlations using modern one-boson exchange potentials (OBE potentials) adjusted to the two-nucleon problem. One possibility in the case of nuclear physics to check the capability of this attempt in a systematic manner is the calculation of the parameters of the Weizsäcker–Bethe formula (WBF). So far, one has concentrated on the symmetric volume properties, which can be calculated in the idealized system of symmetric infinite nulcear matter (INM). In this respect the results are quite encouraging [1,2,4], [9–14]. Systematic theoretical studies of asymmetric nuclear matter (AINM; $N \neq Z$) in this framework, which would test the asymmetric volume parameters of the WBF are, to our knowledge, rare [15–18], and it is the main purpose of this investigation to calculate the properties of AINM as a further step in the described philosophy. Furthermore, one should emphasize that equations of state of asymmetric matter (AEOS) are essential ingredients in star models [19,20] and heavy-ion studies [21].

The first relativistic approach in this framework for calculating INM has been suggested by the Brooklyn group [9], who used a relativistic extension of the Brueckner–Hartree–Fock theory (RBHF). In this pioneering work of Shakin and co-workers [2,9] the problem was treated in the full Dirac space, but the relativistic effect in the determination of the self-consistent basis was taken into account in first-order perturbation theory only. For that reason a comparison with other treatments is rather difficult. The full self-consistency problem in the whole Dirac space as proposed in Refs. [2,12,22] is a tedious problem, and due to its complexity one has tried to avoid this procedure by invoking additional simplifying assumptions. The standard method makes a nonunique ansatz for the scattering matrix T in medium in terms of five Fermi invariants [23] (for instance, in Refs. [12,14] the pseudoscalar invariant is replaced by the pseudovector invariant) and obtains the solution in the c.v. frame only for positive-energy spinors. Once a specific fixed value of the so-called Dirac mass $\tilde{m}$ is chosen and Lorentz boosting mixes only positive-energy helicity spinors among themselves one determines only positive-energy matrix elements in the nuclear matter frame. The consequence of this procedure is that the full matrix structure of T, and hence of the self-energy Σ, is not uniquely determined. It can be shown that the results for Σ depend on the chosen decomposition [24]. An even simpler method was suggested by Brockmann and Machleidt, who avoid this procedure by making the assumption that the scalar and timelike parts of Σ (denoted Σ_s and Σ_0) are momentum independent. From the expression of the positive-energy matrix elements of Σ in the nuclear matter frame in terms of Σ_s and Σ_0 they deduce then in a fit the values for Σ_s

and Σ_0 [4]. Both approaches have been discussed and criticized in full detail in Ref. [22] with the conclusion that a calculation in the full Dirac space, as originally proposed in Ref. [9], seems to be necessary, since all calculations with restriction to positive energy-matrix elements of T lead to ambiguities. Taking these objections into account and in order to clarify the situation we have calculated the properties of INM and AINM for modern OBE potentials in the full Dirac space, and taking the energy-momentum dependence into account. (A drawback of Refs. [9,11,12] is the use of OBE potentials, which are nowadays not considered to be the best choice [24].) With respect to this point we would like to stress that in the case of generalized chemical equilibrium, which is applicable, for instance, in neutron stars, one needs the chemical potential at the Fermi surface for a large density range, and therefore the momentum dependence of the self-energy can be more important than in the case of averaged nuclear properties at saturation [20,25].

As a suitable tool for the treatment we employ the Green's function technique, which is described in great detail in Refs. [12,26,27]. The arrangement of this paper is as follows. In Sec. II we briefly review the relativistic meson-field dynamics in the Green's function theory treated in many-body approximation schemes with dynamical two-body correlations. The results with discussion are given in Sec. III with special emphasis on the outcome for asymmetric matter. Finally in Sec. IV we summarize our conclusions and our outlook for further improvement and applications of the current work.

II. GENERAL THEORY

Since the general theory is outlined in greater detail in Ref. [12] (we refer to equations in Ref. [12] as I.1.1 etc.), we shall only repeat the essential structure of the general scheme and concentrate mainly on some changes due to the asymmetry of the problem.

The dynamics of the system is governed by a Lagrangian density [see equations (I.2.1)–(2.13)]

$$L = L_N + \sum_M (L_M + L_{MN}) \ . \tag{2.1}$$

The three terms describe the noninteracting nucleons, the different free meson fields, and the interaction (independent of $\partial_\mu \psi$). From the field equations one obtains, after elimination of the meson fields, a coupled system of equations for the Green's functions [$G_0 = 1$; the label 1 denotes the time-space coordinates $x_1^0, \vec{x}_1$ and the spin-isospin coordinate $\xi_1(i_1, \alpha_1)$ etc.; we employ the convention to sum or to integrate over all doubly occurring variables]

$$\begin{aligned} G_n(1 \ldots n; 1' \ldots n') = & \sum_{j=1}^{n} (-)^{j+1} G_1^0(1, j') G_{n-1}(2 \ldots n, 1' \ldots \not{j}' \ldots n') \\ & + i\, G_1^0(1,k) \langle km|v|m'm''\rangle G_{n+1}(2 \ldots n\, m'm'', m^+ 1' \ldots n') \end{aligned} \tag{2.2}$$

with the definitions ($\hbar = c = 1; p^\mu \equiv i\partial^\mu$; $|\phi_0\rangle$ denotes the ground-state)

$$G_n(1 \ldots n, 1' \ldots n') = i^n \langle \phi_0 \mid T\{\psi_{\xi_1}(x_1) \ldots \psi_{\xi_n}(x_n) \bar{\psi}_{\xi_n'}(x_n') \ldots \bar{\psi}_{\xi_1'}(x_1')\} \mid \phi_0 \rangle \quad , \tag{2.3}$$

$$[G_1^0(x_1 - x_1')]^{-1} = (-\not{p}_x + m)\delta^4(x - x') \quad , \tag{2.4}$$

and

$$\begin{aligned} \langle 12 \mid v \mid 34 \rangle &= \sum_M \langle 12|v_M|34\rangle \\ &= \sum_M \delta^4(x_1 - x_3)\delta^4(x_2 - x_4) \Gamma^M_{\xi_1\xi_3} \Gamma^M_{\xi_2\xi_4} \Delta^0_M(x_{1'} x_3) \, . \end{aligned} \tag{2.5}$$

The free propagators Δ^0_M and the vertices $\Gamma^M_{\xi_1\xi_2}$ for the different meson fields (s, v, pv,...) are given explicitly in formulas (I.2.18)–(I.2.21) and (I.2.29)–(I.2.33).

The system resembles closely in its formal structure the nonrelativistic case [26,27], and can therefore be decoupled in the same manner. A decoupling procedure was given by Martin and Schwinger, who expressed the system of equations (2.2) as a single functional equation. By an expansion in powers of the source terms one can then incorporate two-body, three-body, and higher correlations in a systematic manner. If one takes only two-body correlations into account and invokes the healing assumption [i.e., terms as $\langle 12|v|34\rangle G_2(34, 1'2')$ are included, but otherwise $G_2(12, 34)$ is replaced by $G_1(1,3)G_1(2,4) - G_1(1,4)G_1(2,3)$; for more details and a comparison between the different approximations, see Refs. [27,28]]; one obtains the so-called ladder-type approximations.

In this scheme one has to treat a coupled system of the Dyson equation for the G function and the effective scattering matrix T in matter

$$\{(G_1^0)^{-1}(1,2) - \Sigma(1,2)\} G_1(2,1') = \delta(1,1') \quad , \tag{2.6}$$

$$\langle 12|T|1'2'\rangle = \langle 12|v|1'2' - 2'1'\rangle + \langle 12|v|34\rangle\Lambda(34,56)\langle 56|T|1'2'\rangle \ , \qquad (2.7)$$

where the self-energy is given by

$$\Sigma(1,2) = -i\langle 14|T|52\rangle G_1(5,4) \quad . \qquad (2.8)$$

The Hartree- or Hartree-Fock approximation is defined by $T = v$ and $T = v_{AS}$, respectively. For the intermediate p-p propagator a standard choice is the Brueckner propagator Λ_B, but one can also use the so-called Λ approximations, defined as (Λ_B is simplified version of Λ^{11} [12,27])

$$-i\Lambda^{ij}(12,34) = \begin{cases} G_1^0(1,3)G_1^0(2,4) \ , \\ \frac{1}{2}[G_1^0(1,3)G_1(2,4) + G_1(1,3)G_1^0(2,4)], \\ G_1(1,3)G_1(2,4) \quad . \end{cases} \qquad (2.9)$$

It turns out that a useful simplification of the treatment can be achieved by utilizing the spectral representation of the Fourier transformed G-function (see I.2.39):

$$G(p) = \int d\omega \frac{A(\vec{p},\omega)}{\omega - (p^0 - \mu)(1 + i\,\eta)} \quad , \qquad (2.10)$$

since all the wanted quantities are determined by the self-energy and the spectral function A alone.

In INM, the spectral function A (and similar G and Σ) takes the form [$\hat{p} \equiv \vec{p}/\mid \vec{p}\mid$]

$$A = A_s(\omega,\vec{p}) + A_v(\omega,\vec{p})(\hat{p}\cdot\vec{\gamma}) + A_v(\omega,\vec{p})\gamma^0 \quad . \qquad (2.11)$$

More explicitly, the final form of A is given by (I.2.58)

$$A(\omega,\vec{p}) = \mathrm{sgn}[\omega_1(\vec{p}) - \Sigma_0(p_0 = \omega_1(\vec{p}),\vec{p})]A^p(\vec{p})\delta(\omega + \mu - \omega^p(\vec{p})) + \mathrm{sgn}[\omega_2(\vec{p}) - \Sigma_0(p_0 = \omega_2(\vec{p}),\vec{p})]A^{ap}(\vec{p})\delta(\omega + \mu - \omega^{ap}(\vec{p})) \ , \qquad (2.12)$$

with the energy-momentum relation for particles (antiparticles; $i = p, ap$):

$$\omega^{(i)} = \Sigma_0\left(\omega^{(i)}(\vec{p}),\vec{p}\right) + (-)^{i+1}\{[m + \Sigma_s(\omega^{(i)}(\vec{p}),\vec{p})]^2 + [\mid \vec{p}\mid + \Sigma_v(\omega^{(i)}(\vec{p}),\vec{p})]^2\}^{1/2} \ . \qquad (2.13)$$

The particle part A^p can be decomposed as follows [$k := \mid \vec{p}\mid ; p_0 = \omega^p(k); \Sigma_s(k) = \Sigma_s(p_0 = \omega^p(k), k)$ etc.]:

$$A_s^p(k) = \frac{m + \Sigma_s(k)}{\mid \frac{\partial F}{\partial \omega}(k)\mid} \quad , \qquad (2.14)$$

$$A_v^p(k) = \frac{k + \Sigma_v(k)}{\mid \frac{\partial F}{\partial \omega}(k)\mid} \quad , \qquad (2.15)$$

$$A_0^p(k) = \frac{\omega^{(p)}(k) - \Sigma_v(k)}{\mid \frac{\partial F}{\partial \omega}(k)\mid} \quad , \qquad (2.16)$$

with

$$F(\omega) := [m + \Sigma_s(\omega,k)]^2 + [k + \Sigma_v(\omega,k)]^2 - [\Sigma_0(\omega,k) - \omega]^2 \quad . \qquad (2.17)$$

Since we use regularized interactions with form factors one can neglect the contributions arising from A^{ap} [4,12].

In AINM one has to distinguish between the proton and neutron parts of the self-energy and the G functions, and one obtains, for instance, the following equations for the protons in an obvious notation (see I.3.27, 3.32):

$$[\not{p} - m - \Sigma^p(p)]_{\alpha_1\alpha_3}G_1^p(p)_{\alpha_3\alpha_2} = -\delta_{\alpha_1\alpha_2} \quad , \qquad (2.18)$$

$$\Sigma^p_{\alpha_1\alpha_2}(k_F^p,k_F^n,p) = \frac{i}{(2\pi)^3}\left\{\int d^3p' \ \theta(\mid \vec{p}' \mid - k_F^p)\langle\alpha_1\,\tfrac{1}{2}p,\alpha_4\,\tfrac{1}{2}\vec{p}' \mid T \mid \alpha_2\,\tfrac{1}{2}p,\alpha_5\,\tfrac{1}{2}p'\rangle A^p_{\alpha_5\alpha_4}(\vec{p}') + \int d^3p'\theta(\mid \vec{p}' \mid - k_F^n)\langle\alpha_1\,\tfrac{1}{2}p,\alpha_4 - \tfrac{1}{2}p' \mid T \mid \alpha_2\,\tfrac{1}{2}p,\alpha_5 - \tfrac{1}{2}p'\rangle A^n_{\alpha_5\alpha_4}(\vec{p}')\right\} . \qquad (2.19)$$

For the neutrons one gets similar equations. For the calculation of the six matrix elements of the self-energy one needs 18 T-matrix elements with respect to isospin. In the case of symmetric INM one gets along with a summation over the isospin channels, but in the case of AINM one is forced, due to the different self-energies for p and n, to calculate separately the T-matrix elements for the different isospin degrees (i.e., $\langle pp \mid T \mid pp \rangle$, $\langle nn \mid T \mid nn \rangle$, $\langle pn \mid T \mid pn \rangle$), which are determined via coupled integral equations. These features render the numerical procedure for AINM much more complicated than for symmetric INM [29].

In both cases the main obstacle is the treatment in the full Dirac space, for which one needs a self-consistent basis, which decouples the integral equations for the T matrix and makes the one-body propagator diagonal. This procedure is described in detail in Secs. III C and IV A of Ref. [12].

In the self-consistent iteration procedure one starts, for instance, with the outcome of the HF treatment for Σ and determines in the first step the spectral functions A, the momentum densities $n(p)$ (see I.3.50) and the energy-momentum relations $\omega(k)$. After solving the T-matrix equations one obtains via Eqs. (2.12)–(2.17) and (2.19) new values for the self-energy, which can be used in the next iteration step. The connection between the matrix elements in the self-consistent basis and the decomposition in Σ_s, Σ_v, and Σ_0 is given, for instance, for Σ_s, by [$\phi\,(\theta)$ denote the positive (negative) energy helicity eigenspinors; for Σ_0, Σ_v, see (I.3.35)–(I.3.46) and [29]]:

$$\Sigma_s^i(p) = \frac{1}{2}\left\{\Sigma^i_{\phi\phi}(p) - \Sigma^i_{\theta\theta}(p)\right\} \text{ etc.} \tag{2.20}$$

With the final results, one can determine the energy and baryon density of AINM, given as ($k := \mid \vec{p} \mid$)

$$\epsilon = \frac{1}{4\pi^3}\int d^3p\{\theta(k_F^p - k)(2\,[m^p A_s^p(k) - kA_v^p] + [\Sigma_s^p(p)A_s^p(k) - \Sigma_v^p(p)A_v^p(k) + \Sigma_0^p(p)A_0^p(k)]_{p^0=\omega^p(k)}) + (p \leftrightarrow n)\} \tag{2.21}$$

and

$$\rho = \frac{4}{(2\pi)^3}\int d^3p\,\{\theta(k_F^p - k)A_0^p(k) + (p \leftrightarrow n)\} \quad . \tag{2.22}$$

The chemical potentials for proton and neutrons defined by

$$\mu^{p,n} = \omega^{p,n}(k_F^{p,n}) = \Sigma_0^{p,n}(\omega^{p,n}(k_F^{p,n}), k_F^{p,n}) + \sqrt{[m + \Sigma_s^{p,n}(\omega^{p,n}(k_F^{p,n}), k_F^{p,n})]^2 + [k_F^{p,n} + \Sigma_v^{p,n}(\omega^{p,n}(k_F^{p,n}), k_F^{p,n})]^2} \tag{2.23}$$

are more sensitive to the momentum dependence. Since they are important for the determination of the β equilibrium of hadronic matter in neutron stars, it is advantageous to determine the full momentum dependence of the self-energies [20,25]. By utilizing the definitions

$$\rho = \rho^p + \rho^n \quad , \tag{2.24}$$

$$\delta = \frac{\rho^n - \rho^p}{\rho} \quad , \tag{2.25}$$

one can express the energy per particle as a function of the total baryon density ρ and the asymmetry δ. The mass formula reads as [ρ_{00} denotes the equilibrium (saturation) density of symmetric INM]

$$e(\rho,\delta) = (a_v + \frac{1}{18}K_v\epsilon^2 + \cdots) + \delta^2\left(J + \frac{1}{3}L\,\epsilon + \frac{1}{18}K_{\rm sym}\epsilon^2 + \cdots\right) \quad , \tag{2.26}$$

where $\epsilon := (\rho - \rho_{00})/\rho_{00}$. K_v is the compression modulus of symmetric INM:

$$K_v = 9\,\rho^2\left(\frac{\partial^2 e}{\partial\rho^2}\right)_{\rho=\rho_{00},\delta=0} \quad . \tag{2.27}$$

J denotes the bulk symmetry energy of the semiempirical mass formula, which is equal to the symmetry energy

$$e_{\rm sym}(\rho) := \frac{1}{2}\frac{\partial^2 e(\rho,\delta)}{\partial\delta^2}\bigg|_{\delta=0} \tag{2.28}$$

at saturation density ρ_{00}. L and $K_{\rm sym}$ are related to the slope and curvature of the symmetry energy, respectively, at density ρ_{00}:

$$L = 3\rho\left(\frac{\partial e_{\rm sym}}{\partial\delta}\bigg|_{\rho=\rho_{00}}\right) \quad , \tag{2.29}$$

$$K_{\rm sym} := 9\,\delta^2\left(\frac{\partial^2 e_{\rm sym}}{\partial\rho^2}\bigg|_{\rho=\rho_{00}}\right) \quad . \tag{2.30}$$

For small δ one obtains the approximate formulas for the equilibrium values

$$\rho_{eq}^{(\delta)} \simeq \rho_{00}\left(1 - \frac{3L}{K_v}\delta^2\right) \quad , \tag{2.31}$$

$$e(\rho_{eq}, \delta) \simeq a_v + J\,\delta^2 \quad . \tag{2.32}$$

III. RESULTS AND DISCUSSION

A. General remarks

For this investigation we have selected modern OBE potentials constructed by Brockmann and Machleidt, which have been widely used in more recent relativistic treatments. They adjusted three different potentials to the two-nucleon data, denoted by A, B, and C, which differ mainly by the strength of the tensor force increasing from A to C. Since the tensor force determines the location of the saturation point, it is advantageous for the construction of the Coester band, to consider different potentials. Since these potentials were not available at the time of our first investigation, we have repeated the calculations for these potentials for the case of symmetric INM, too. Furthermore, we used two OBE potentials given by the Groningen group. As explained in the Introduction and outlined in Sec. II, we perform the calculations in the whole Dirac space and neither use the assumption of expressing T in terms of five Fermi invariants, as suggested by J.A. McNeil, J.R. Shephard, and S. Wallace [23], which may lead, depending on the decomposition, to different results for the self-energy, nor use the fitting procedure of Ref. [24], where one invokes the assumptions of constant self-energies Σ_s and $\Sigma_0(\Sigma_v = 0)$ in the system of equations for Σ, which reads in full generality as follows: $[W(p) := \sqrt{\tilde{m}^2(p) + \tilde{k}^2};\ \tilde{m}(p) = m + \Sigma_s(p);\ \tilde{k} = k + \Sigma_v(p)]$:

$$\Sigma_{\phi\phi}(p) = \Sigma_s(p) + \frac{\tilde{k}(p)}{\tilde{m}(p)}\Sigma_v(p) + \frac{W(p)}{\tilde{m}(p)}\Sigma_0(p) \quad , \tag{3.1}$$

$$\Sigma_{\theta\theta}(p) = -\Sigma_s(p) + \frac{\tilde{k}(p)}{\tilde{m}(p)}\Sigma_v(p) + \frac{W(p)}{\tilde{m}(p)}\Sigma_0(p) \quad , \tag{3.2}$$

$$\Sigma_{\theta\phi}(p) = \frac{W(p)}{\tilde{m}(p)}\Sigma_v(p) + \frac{\tilde{k}(p)}{\tilde{m}(p)}\Sigma_0(p) \quad , \tag{3.3}$$

and determines the constant Σ_s and Σ_0 via a fit procedure from the positive energy spinor matrix elements of $\Sigma_{\phi\phi}$ alone. For these reasons it is difficult to compare the results directly. However, in order to obtain some similarity with the Brockmann procedure, we tried also a simplified version, denoted by RBHF$^{(2)}$, in which we use an iteration procedure, where we always replace in the iteration the momentum dependent self-energies by the momentum averaged self-energies. Self-consistency in this case is obtained, if the averaged self-energies stays constant. This method is by far less time consuming than the iteration procedure, in which the full momentum dependence is taken into account (RBHF$^{(1)}$).

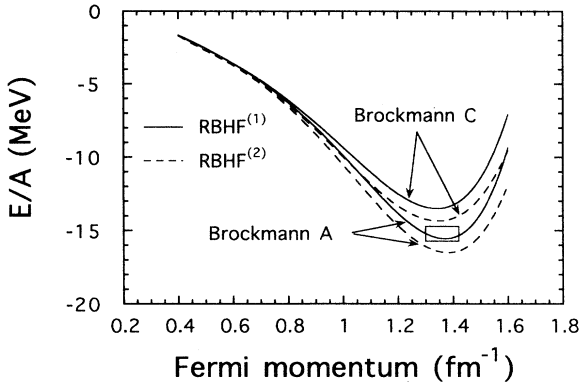

FIG. 1. Binding energy per nucleon versus Fermi momentum for symmetric INM in RBHF for the Brockmann potentials A and C. The solid (dashed) curves correspond to the treatment with (averaged) momentum dependency of the self-energies. The square indicates the empirical range.

B. Symmetric infinite nuclear matter

The comparison for the different Brockmann potentials for symmetric INM are given in Table I. The energy per particle for INM is exhibited in Fig. 1 for the potentials A and C (for B, see Ref. [17]). The agreement of the saturation properties with the results of Brockmann

TABLE I. Saturation properties of symmetric INM for different approximations for the three Brockmann potentials A, B, C [4]: RBHF$^{(1)}$ (full basis; momentum dependent self-energy), RBHF$^{(2)}$ (full basis; momentum-averaged self-energy), RBHF$^{(3)}$ (positive energy spinors only; momentum independent self-energy [4]); $\Lambda^{00(2)}$ approximation). For comparison we give also the outcome of the relativistic HF approximation, where ρ and E/A are adjusted and the properties of asymmetric matter were calculated [15]: RHF$^{(1)}$ (σ, ω mesons only), RHF$^{(2)}$ (σ, ω, π, and ρ mesons; $f_\rho/g_\rho = 6.6$), RHF$^{(3)}$ (σ, ω, π, and ρ-mesons; $f_\rho/g_\rho = 3.7$).

Method	E/A (MeV)	ρ_{00} (fm^{-3})	k_F (fm^{-1})	K_v (MeV)
RBHF$^{(1)}$(A)	-15.72	0.174	1.37	336
RBHF$^{(2)}$(A)	-16.49	0.174	1.37	280
RBHF$^{(3)}$(A)	-15.59	0.185	1.40	290
$\Lambda^{00(2)}$(A)	-23.51	0.215	1.47	297
RBHF$^{(1)}$(B)	-14.81	0.170	1.36	264
RBHF$^{(2)}$(B)	-15.73	0.172	1.365	249
RBHF$^{(3)}$(B)	-13.60	0.174	1.37	249
$\Lambda^{00(2)}$(B)	-21.90	0.210	1.46	260
RBHF$^{(1)}$(C)	-13.73	0.162	1.34	268
RBHF$^{(2)}$(C)	-14.38	0.170	1.36	258
RBHF$^{(3)}$(C)	-12.26	0.155	1.32	185
$\Lambda^{00(2)}$(C)	-20.57	0.206	1.45	293
RHF$^{(1)}$	-15.75	0.148		610
RHF$^{(2)}$	-15.75	0.148		360
RHF$^{(3)}$	-15.75	0.148		460

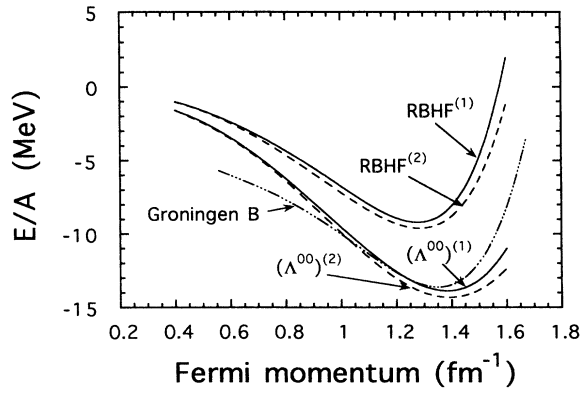

FIG. 2. Comparison of the binding energy per nucleon in INM for the treatment in the full Dirac space [RBHF$^{(1)}$ and $\Lambda^{00(1)}$ full curves, RBHF$^{(2)}$ and $\Lambda^{00(2)}$ dashed curves; the superscripts "1" and "2" denote the version with full and averaged momentum dependence, respectively (see text)] with the treatment utilizing the decomposition of the scattering amplitude T into five Fermi invariants (dashed–dotted curve; Groningen potential B; for more details, see text).

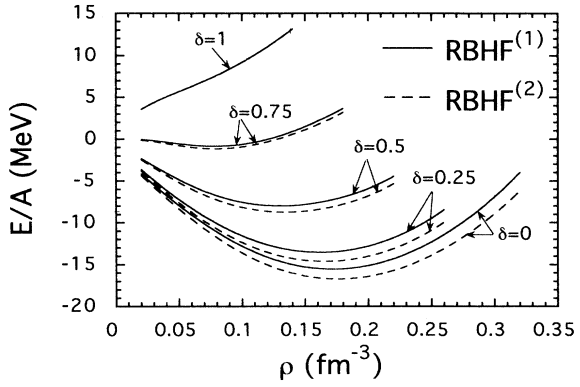

FIG. 3. Binding energy per nucleon versus density for different asymmetries in the RBHF approximation (Brockmann potential A).

and Machleidt is rather good. In our approach we obtain a little more binding, and the saturation density varies less. We have also calculated the nuclear matter properties within the Λ^{00} approximation, which is the simplest Λ approximation. This approximation is known to give more binding than the RHBF approximation [12]. This feature is certified in our calculations (see Tables I and II). Unfortunately we could not treat for AINM, due to limited numerical capabilities, the more interesting other Λ approximations and therefore we restricted ourselves to the described RBHF and Λ^{00} approximations. The results for the Groningen potential B are given in Table II. A comparison with the calculation of the nuclear matter parameter with the treatment of Ref. [10] (T is decomposed in five Fermi invariants) is given in Fig. 2 for the Groningen potential B, which shows that the differences due to the calculation schemes are slightly larger in this case.

C. Asymmetric matter

1. Bulk properties

We turn now to the interesting case of asymmtric matter. The outcome for the energy per nucleon for the Brockmann potentials A and C (we concentrate on the potentials A and C, since some results for B are already given in Ref. [17]) as a function of the baryon density for different asymmetries is displayed in Figs. 3 and 4. First, one recognizes the expected result that for neutron matter ($\delta = 1$) the results are almost identical, since the different tensor forces are not relevant in this case. In Fig. 5 we give E/A results for the Λ^{00} approximation (Brockmann A). In a recent preprint the properties of asymmetric matter were calculated for the potential A utilizing the Brockmann-Machleidt assumptions and a different Pauli operator [18], which makes a direct comparison difficult. A comparison of the E/A curves (the asymmetry parameters are not given) shows an agreement similar as in the original Brockmann calculations for symmetric matter. For instance, the deviation for pure neutron matter at nuclear matter saturation is approximately 2 MeV.

Of further interest are the energies per particle at equilibrium as a function of the asymmetry, displayed in

TABLE II. Saturation properties of symmetric INM for the Groningen potential B.

Method	E/A (MeV)	ρ_{00} (fm^{-3})	k_F (fm^{-1})	K_v (MeV)
RBHF$^{(1)}$	-9.21	0.145	1.29	191
RBHF$^{(2)}$	-9.68	0.152	1.31	183
$\Lambda^{00(1)}$	-13.92	0.181	1.39	264
$\Lambda^{00(2)}$	-14.53	0.189	1.41	178

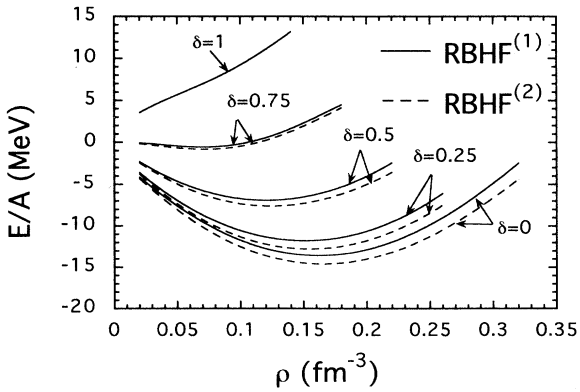

FIG. 4. Binding energy per nucleon versus density for different asymmetries in the RBHF approximation (potential C).

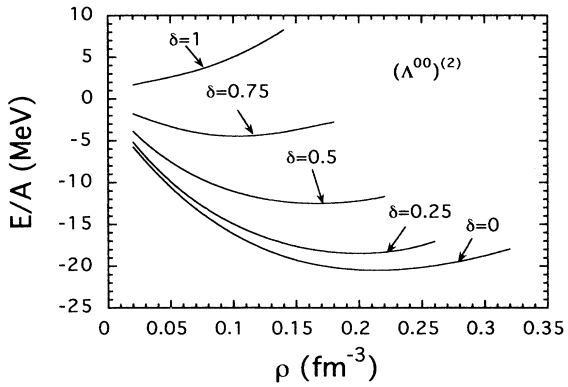

FIG. 5. Binding energy per nucleon versus density for different asymmetries in the Λ^{00} approximation (potential C).

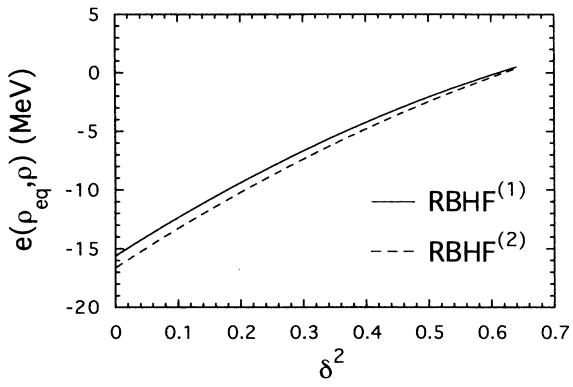

FIG. 6. Energy per particle at equilibrium as function of asymmetry (potential A).

Fig. 6 and symmetry energy shown in Fig. 7 (potential A). The curves show the same behavior as in the relativistic Hartree-Fock treatment, however the qualitative features are quite different from the nonrelativistic treatment with Skyrme forces (S III), where, for instance, the symmetry energy bends over at densities of approximately 0.15 fm^{-3} [15]. The properties of INM and AINM are listed in Table III and compared with the outcome of relativistic Hartree and Hartree-Fock calculations, and with nonrelativistic treatments [15,30]. As mentioned before the agreement of the bulk properties with the accepted values of the mass formula is quite satisfactory. Also the value of the asymmetry parameter J is located within the accepted boundaries. The values for L and $K_{\rm sym}$, which are much more uncertain, lie between the values of the relativistic Hartree parametrization NL-SH and the Skyrme parametrization SkM* and conform nicely to the systematics already established in nonrelativistic fits to nuclear data, for instance, increasing values of J are associated with increasing values of L [31]. In such a comparison one has to keep in mind that despite the fact that these parametrizations have been used very often in the past, they still have some deficiencies (see, for instance, Refs. [30,32,33]). One expects from a comparison between SkM* and NL-SH due to the different values of J for L and $K_{\rm sym}$ values located between the corresponding values for these parametrizations, which is verified by our calculation. Finally we test the validity of the quadratic approximation for the symmetry energy

$$e(\rho,\delta) = e(\rho,0) + e_{\rm sym}(\rho)\delta^2 \quad . \tag{3.4}$$

This approximation holds also in the nonrelativistic

TABLE III. Properties of symmetric and asymmetric nuclear matter in the RBHF approximation (RBHF$^{(2)}$) for the Brockmann potentials A, B and C. For comparison the corresponding values are also given for phenomenological relativistic Hartree and Hartree-Fock, and nonrelativistic Skyrme force calculations. For the Hartree calculations we selected some currently used parameter sets, namely LN1, and NL-SH. The HF results were taken from Ref. [15]. SkM* and S III denote two well known Skyrme forces, FRDM is the latest and most sophisticated of the droplet-model mass formulas, while ETFSI-1 denotes the first mass formula to be based entirely on microscopic forces (for more details, see Ref. [30]). The saturation density ρ_{00} is given in fm^{-3}. All other quantities are in MeV.

	E/A	ρ_{00}	K_v	J	L	$K_{\rm sym}$
Br A	-16.49	0.174	280	34.4	81.9	-66.4
Br B	-15.73	0.172	249	32.8	90.2	9.97
Br C	-14.38	0.170	258	31.5	76.1	-35.1
RHF$^{(1)}$	-15.75	0.148	610.0	28.9	132	466
RHF$^{(2)}$	-15.75	0.148	360.0	43.3	135	105
RHF$^{(3)}$	-15.75	0.148	460.0	38.6	138	276
NL 1	-16.423	0.1519	211.7	43.49	140.2	143.0
NL-SH	-16.346	0.1460	355.8	36.13	113.7	79.82
SkM*	-15.776	0.1603	216.7	30.03	45.8	-155.9
SIII	-15.857	0.1453	355.4	28.16	9.9	-393.7
FRDM	-16.247	0.1529	240	32.73	0	-
ETFSI-1	-15.87	0.1607	234.7	27.0	-9.29	-336.8

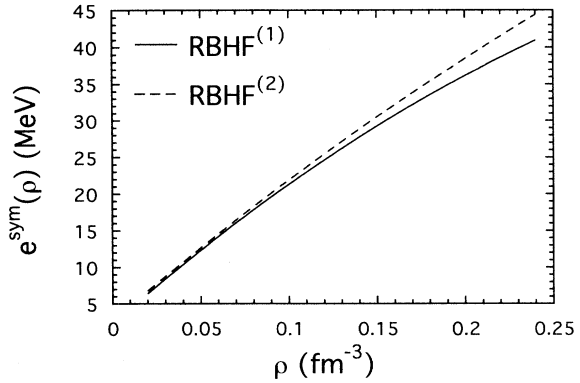

FIG. 7. Symmetry energy as function of the density (potential A). For the saturation density the values of the curves give the bulk symmetry energy J.

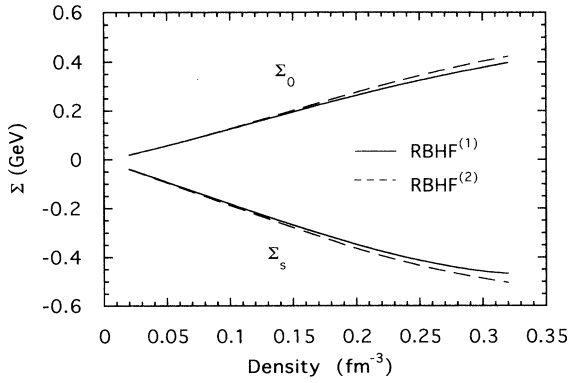

FIG. 9. Comparison of the density dependence of the scalar and timelike part of the self-energy in symmetric INM with full (RBHF$^{(1)}$) and averaged (RBHF$^{(2)}$) momentum dependence (see text; potential B).

Brueckner approximation [34]. From Fig. 8 one can see that this presumption is also fulfilled to a very high degree in the RBHF approximation.

2. *Self-energies*

If one compares in symmetric INM the momentum averaged approximation RBHF$^{(2)}$ with the nonaveraged approximation RBHF$^{(1)}$, one obtains a decrease (increase) for $\Sigma_s(\Sigma_0)$ for RHBF$^{(1)}$, which is shown in Fig. 9. This effect increases with density, and can be understood by the fact that near the Fermi momentum $\Sigma_0(\Sigma_s)$ decreases (increases). By momentum averaging one suppresses this effect and obtains the described differences. However, for the calculation of the EOS for asymmetric matter in β equilibrium, important for neutron stars, where one needs the single-particle energy at the top of the Fermi sea at higher densities, this effect is not negligible [see Eq. (2.23)]. The Dirac masses, defined as $\tilde{m} = m + \Sigma_s(p_F) \approx 0.66$ m (potentials A, B, C) are larger than in the Brockmann approximation (≈ 0.62 m), and the density dependence differs too. (Density-dependent parametrizations of the self-energies have been applied with some success in finite nuclear structure calculations [36,37]. A comparison within the extended Thomas-Fermi scheme, which gives *a priori* smaller radii, shows no clear conclusions with respect to the density dependence, since either the energies or the radii are better reproduced by the parametrizations of the different INM schemes. For the finite nuclei the choice of the σ mass may be of greater importance, where one may have some freedom since INM is mainly influenced by the ratio g_σ/m_σ [36,39]. This seems also to be certified by the poor reproduction of the surface properties of semi-infinite nuclear matter utilizing the Brockmann parametrization; for more details, see Refs. [33,38,39].)

For asymmetric nuclear matter the density dependence for several asymmetries is exhibited in Figs. 10 and 11.

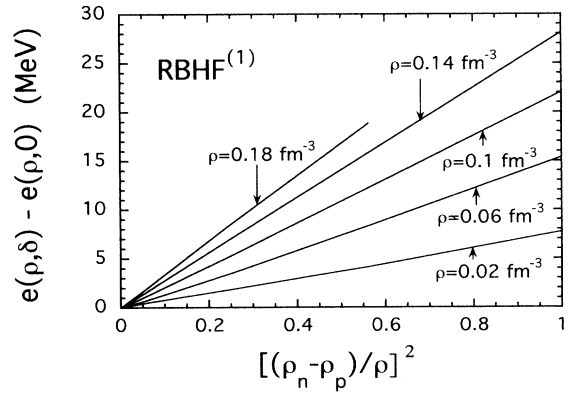

FIG. 8. Test of the quadratic approximation of the symmetry energy: Asymmetry energy per nucleon in the RBHF$^{(1)}$ approximation in the range $0 \leq \delta^2 \leq 1$ at five densities. The slope of each curve gives the corresponding symmetry energy (potential A).

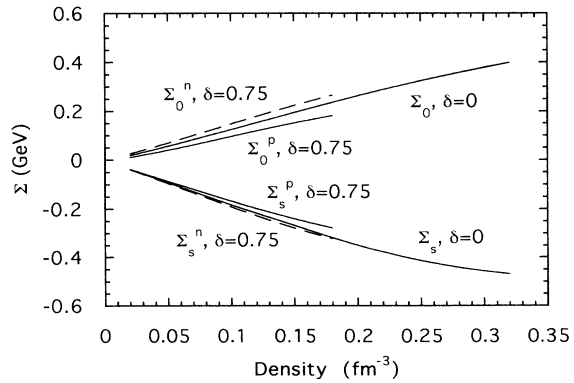

FIG. 10. Density dependence of the self-energies for protons and neutrons for different asymmetries in the RBHF$^{(1)}$ approximation (potential B).

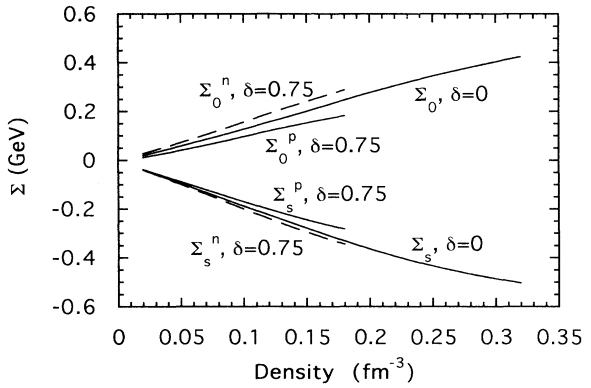

FIG. 11. Density dependence of the self-energies for protons and neutrons for different asymmetries in the RBHF$^{(2)}$ approximation (potential B).

As already expected from the direct term, Σ_0^n and Σ_0^p, respectively, increase and decrease with δ approximately by the same amount. For the differences in the scalar parts the main source for the difference is hidden in a more complex manner in the exchange contributions (the pure Hartree theory gives $\Sigma_s^p = \Sigma_s^n$). A closer inspection of the Fock terms in RHF reveals that the contributions for ρ, δ, π mesons to the proton self-energy are larger than for the neutron self-energy [29]. For pure neutron matter the Fock contribution for Σ^p is twice as large as the contribution for Σ^n. Therefore one expects, as demonstrated in Fig. 10, larger deviations for Σ_0 with δ and relative small changes in Σ_s, where Σ_s^p is stronger influenced by the asymmetry as Σ_s^n.

IV. SUMMARY AND OUTLOOK

Relativistic nuclear matter calculations with inclusion of dynamical two-body correlations require the knowledge of the effective scattering matrix in the nuclear-matter frame. For a complete determination in a nonambiguous manner, the complete representation of the NN amplitude in the full Dirac space is needed. We have solved this problem utilizing the method described in Refs. [12,29], so avoiding the ambiguous procedures, which are restricted to the positive-energy sector only [4,10,14]. For the interaction we used three modern OBE potentials constructed by Brockmann and Machleidt. The potentials differ mainly with respect to the tensor force. For that reason one expects differences for symmetric matter, but for pure neutron matter the properties should be almost identical, which is certified by our calculations. The bulk properties of symmetric infinite matter are in good agreement with the semiempirical values. In the next step we extended the calculations to the properties of asymmetric matter in order to test the predictive power of this parameter-free theory. Such an extension seems to be a natural systematical step towards the capability of the approach to describe nuclear properties, since a test bench in this respect is the reproduction of the semiempirical values of the mass formula. The obtained results for the bulk symmetry energy agree well with the empirical values, and also the values for the asymmetry slope and the asymmetry curvature fit nicely in the expected pattern.

The binding energy at saturation decreases approximately as a quadratic function of the asymmetry parameter δ, and the system becomes unbound at $\delta = 0.67$. The symmetry energy as a function of the density is as in the RHF treatment less curved as in the nonrelativistic treatments. Furthermore, we could confirm the empirical parabolic law of the binding energy as function of the density for higher asymmetries. Additionally we have studied the impact of using momentum-independent self-energies. For densities below the nuclear matter saturation density the differences are small, but for higher densities, relevant, for instance, for the EOS in generalized β equilibrium in neutron stars, the differences are not negligible.

In summary, we have investigated the properties of symmetric and antisymmetric nuclear matter by solving self-consistently the relativistic many-body problem with two-body correlations in the RBHF and Λ^{00} approximation, using modern OBE potentials. The results for the bulk properties of symmetric as well as asymmetric matter are in rather good agreement with the semiempirical values of the mass formula, which gives additional hope that the relativistic theory with inclusion of correlations might be capable "of understanding" nuclear systems in a parameter-free manner.

ACKNOWLEDGMENT

We would like to thank R. Brockmann for useful conversations.

[1] B.D. Serot and J.D. Walecka, Adv. Nucl. Phys. **16**, 1 (1986), and references therein.
[2] L.S. Celenza and C.M. Shakin, *Relativistic Nuclear Physics* (World Scientific, Singapore 1986), and references therein.
[3] E.D. Cooper, S. Hama, B.C. Clark, and R.L. Mercer, Phys. Rev. C **47**, 297 (1993), and references therein.
[4] R. Brockmann and R. Machleidt, Phys. Rev. C **42**, 1965 (1990).
[5] P.G. Reinhard, Rep. Prog. Phys. **52**, 439 (1989), and references therein.
[6] Y.K. Gambhir, P. Ring, and A. Thimet, Ann. Phys. (N.Y.) **189**, 132 (1990).
[7] M.M. Sharma, M.A. Nagarajan, and P. Ring, Phys. Lett. B **312**, 377 (1993).
[8] Jian-Kang Zhang, Yante Jin, and D.S. Onley, Phys. Rev. C **48**, 2697 (1993).
[9] M.R. Anastasio, L.S. Celenza, and C.M. Shakin, Phys.

Rev. C **23**, 2258 (1981); **23**, 2273 (1981).
[10] J.B. TerHaar and R. Malfliet, Phys. Rep. **149**, 209 (1987).
[11] C.J. Horowitz and B.D. Serot, Nucl. Phys. **A464**, 613 (1987).
[12] P. Poschenrieder and M.K. Weigel, Phys. Rev. C **38**, 471 (1988); Phys. Lett. B **200**, 231 (1988).
[13] A. Amorin and J.A. Tjon, Phys. Rev. Lett. **68**, 772 (1992).
[14] F. de Jong and R. Malfliet, Phys. Rev. C **44**, 998 (1991).
[15] M. Lopez-Quelle *et al.*, Nucl. Phys. **A483**, 479 (1988).
[16] H. Müther, M. Prakash, and T.L. Ainsworth, Phys. Lett. B **199**, 469 (1987).
[17] H. Huber, F. Weber, and M.K. Weigel, Phys. Lett. B **317**, 485 (1993); "The relativistic treatment of symmetric and asymmetric nuclear matter," in *Hot and Dense Nuclear Matter*, Proceedings of the NATO Advanced Study Institute, Bodrum/Turkey, 1993, edited by W. Greiner, H. Stöcker, and A. Gallmann (Plenum Press, New York, 1994).
[18] L. Engvik, M. Hjorth-Jensen, E. Osnes, G. Bao, and E. Østgard; "Asymmetric nuclear matter and neutron star properties," Report No. UIO/PHYS/94-12, University of Oslo, 1994 (unpublished).
[19] G.E. Brown, Phys. Rep. **163**, 1 (1988), and references therein.
[20] F. Weber and N.K. Glendenning, "Rotating Relativistic Neutron Stars;" in Proceedings of the Nankai Summer School, *Astrophysics and Neutrinophysics*, Tianjin, 1991, edited by D.H. Feng, G.Z. He, and X.Q. Li (World Scientific, Singapore, 1993), and references therein.
[21] P. Stock, Phys. Rep. **135**, 259 (1986), and references therein.
[22] C. Nuppenau, Y.J. Lee, and A.D. Mac Kellar, Nucl. Phys. **A504**, 839 (1989), and references therein.
[23] J.A. McNeil, L. Ray, and S.J. Wallace, Phys. Rev. C **27**, 2123 (1983).
[24] R. Machleidt, K. Holinde, and Ch. Elster, Phys. Rep. **149**, 1 (1987).
[25] H. Huber, F. Weber, and M.K. Weigel, Phys. Rev. C **50**, R 1287 (1994).
[26] P.C. Martin and J. Schwinger, Phys. Rev. **115**, 1342 (1959).
[27] M. Weigel and G. Wegmann, Fortschr. Phys. **19**, 451 (1971), and references therein.
[28] R. Puff, A.S. Reiner, and L. Wilets, Phys. Rev. **149**, 778 (1968).
[29] H. Huber, "Die relativistische Zustandsgleichung für symmetrische und asymmetrische Kernmaterie und ihr Einfluß auf die Eigenschaften von Neutronensternen," Diploma-Thesis, Munich, 1993.
[30] D. Von-Eiff, J.M. Pearson, W. Stocker, and M.K. Weigel, Phys. Lett. B **324**, 279 (1994).
[31] M. Farine, J. Coté, and J.M. Pearson, Phys. Rev. C **24**, 303 (1981), and references therein.
[32] D. Von-Eiff, J.M. Pearson, W. Stocker, and M.K. Weigel, Phys. Rev. C **50**, 831 (1994).
[33] D. Von-Eiff, W. Stocker, and M.K. Weigel, Phys. Rev. C **50**, 1436 (1994).
[34] I. Bombaci and U. Lombardo, Phys. Rev. C **44**, 1982 (1991).
[35] S. Marcos, M. Lopez-Quelle, and N. Van Giai, Phys. Lett. B **257**, 5 (1991).
[36] R. Brockmann and H. Toki, Phys. Rev. Lett. **68**, 3408 (1992).
[37] S. Haddad and M.K. Weigel, Phys. Rev. C **48**, 2740 (1993).
[38] S. Haddad (private communication).
[39] S. Haddad and M.K. Weigel, Nucl. Phys. **A578**, 471 (1994).